3. Mohler, H. & Okada, T. Benzodiazepine receptor: demonstration in the central nervous system. *Science* **198,** 849–851 (1977).
4. Braestrup, C., Albrechtsen, R. & Squires, R. F. High densities of benzodiazepine receptors in human cortical areas. *Nature* **269,** 702–704 (1977).
5. Wieland, H. A., Lüddens, H. & Seeburg, P. H. A single histidine in $GABA_A$ receptors is essential for benzodiazepine agonist binding. *J. Biol. Chem.* **267,** 1426–1429 (1992).
6. Kleingoor, C., Wieland, H. A., Korpi, E. R., Seeburg, P. H. & Kettenmann, H. Current potentiation by diazepam but not GABA sensitivity is determined by a single histidine residue. *Neuroreport* **4,** 187–190 (1993).
7. Benson, J. A., Löw, K., Keist, R., Mohler, H. & Rudolph, U. Pharmacology of recombinant γ-aminobutyric $acid_A$ receptors rendered diazepam-insensitive by point-mutated α-subunits. *FEBS Lett.* **431,** 400–404 (1998).
8. Fritschy, J.-M. *et al.* Five subtypes of type A γ-aminobutyric acid receptors identified in neurons by double and triple immunofluorescence staining with subunit-specific antibodies. *Proc. Natl Acad. Sci. USA* **89,** 6726–6730 (1992).
9. Lakso, M. *et al.* Efficient *in vivo* manipulation of mouse genomic sequences at the zygote stage. *Proc. Natl Acad. Sci. USA* **93,** 5860–5865 (1996).
10. Knoflach, F. *et al.* Pharmacological modulation of the diazepam-insensitive recombinant γ-amino-butyric $acid_A$ receptors α4β2γ2 and α6β2γ2. *Mol. Pharmacol.* **50,** 1253–1261 (1996).
11. Bernard, F. *et al.* in *Zolpidem: an Update of its Pharmacological Properties and the Therapeutic Place in the Management of Insomnia* (eds Freeman, H., Puech, A. J. & Roth, T.) 21–31 (Elsevier, Paris, 1996).
12. Melchior, C. L. & Allen, P. M. Interaction of pregnanolone and pregnanolone sulfate with ethanol and pentobarbital. *Pharmacol. Biochem. Behav.* **42,** 605–611 (1992).
13. Beuzen, A. & Belzung, C. Link between emotional memory and anxiety states: a study by principal component analysis. *Physiol. Behav.* **58,** 111–118 (1995).
14. Vogel, J. R., Beer, B. & Clody, D. E. A simple and reliable conflict procedure for testing anti-anxiety agents. *Psychopharmacology* **21,** 1–7 (1971).
15. Bonetti, E. P. *et al.* Benzodiazepine antagonist Ro 15-1788: neurological and behavioral effects. *Psychopharmacology* **78,** 8–18 (1982).
16. Hunkeler, W. *et al.* Selective antagonists of benzodiazepines. *Nature* **290,** 514–516 (1981).
17. Bonetti, E. P. *et al.* Ro 15-4513: Partial inverse agonism at the BZR and interaction with ethanol. *Pharmacol. Biochem. Behav.* **31,** 733–749 (1988).
18. Misslin, R., Belzung, C. & Vogel, E. Behavioural validation of a light/dark choice procedure for testing anti-anxiety agents. *Behav. Proc.* **18,** 119–132 (1989).
19. Lister, R. G. The use of a plus-maze to measure anxiety in the mouse. *Psychopharmacology* **92,** 180–185 (1987).

Supplementary information is available on *Nature*'s World-Wide Web site (http://www.nature.com) or as paper copy from the London editorial office of *Nature*.

Acknowledgements

We thank Y. Lang for blastocyst injections, D. Blaser, S. Ganz, H. Pochetti and G. Schmid for animal care, R. Keist and C. Michel for technical assistance and H. Westphal for providing Ella-cre mice. This work was supported by a grant from the Swiss National Science Foundation.

Correspondence and requests for materials should be addressed to U.R. (e-mail: rudolph@pharma.unizh.ch).

P/Q-type calcium channels mediate the activity-dependent feedback of syntaxin-1A

Kathy G. Sutton*†, John E. McRory*†, Heather Guthrie*, Timothy H. Murphy‡ & Terrance P. Snutch*

** Biotechnology Laboratory and ‡ Kinsmen Laboratory of Neurological Research, Dept Psychiatry University of British Columbia, Vancouver, V6T 1Z3, Canada*
† These authors contributed equally to this work.

Spatial and temporal changes in intracellular calcium concentrations are critical for controlling gene expression in neurons[1–5]. In many neurons, activity-dependent calcium influx through L-type channels stimulates transcription that depends on the transcription factor CREB by activating a calmodulin-dependent pathway[6–11]. Here we show that selective influx of calcium through P/Q-type channels[12–14] is responsible for activating expression of syntaxin-1A, a presynaptic protein that mediates vesicle docking, fusion and neurotransmitter release. The initial P/Q-type calcium signal is amplified by release of calcium from intracellular stores and acts through phosphorylation that is dependent on the calmodulin-dependent kinase CaM K II/IV, protein kinase A and mitogen-activated protein kinase kinase. Initiation of syntaxin-1A expression is rapid and short-lived, with syntaxin-1A ultimately interacting with the P/Q-type calcium channel to decrease channel availability. Our results define an activity-dependent feedback pathway that may regulate synaptic efficacy and function in the nervous system.

Syntaxin-1A interacts with the synaptic core (SNARE) complex and is tightly regulated by a number of proteins including munc-13, munc-18 and tomosyn[15–18]. Syntaxin-1A also binds to the domain II–III linker of N- and P/Q-type voltage-gated Ca^{2+} channels and shifts current inactivation properties to more negative potentials[19–23]. Transient expression of human α_{1A} (P/Q-type) Ca^{2+} channels in HEK293 cells resulted in a relatively negative steady-state inactivation (SSI) and indicated that there may be a corresponding interaction with syntaxin (Fig. 1a; voltage for 50% inactivation ($V50_{inact}$) $= -69.2 \pm 1.6$ mV, $n = 17$). Incubation with botulinum toxin C1 (200–400 ng ml^{-1} for 24 h) to cleave syntaxin[24] made the SSI ~10 mV more depolarized (Fig. 1a; $V50_{inact} = 59.7 \pm 1.7$ mV, $P < 0.001$, $n = 11$). Treatment with botulinum C1 toxin did not affect the voltage-dependence of current activation (Fig. 1a inset). To confirm the presence of syntaxin, cells were co-transfected with an antisense syntaxin construct directed against the first 338 bases of rat syntaxin (GenBank accession code M95734; 90% identical with human syntaxin-1A), which resulted in a depolarizing shift in the SSI curve (Fig. 1b; $V50_{inact} = -63.1 \pm 1.3$ mV, $P < 0.01$, $n = 18$). Thus, syntaxin-1A endogenous to HEK293 cells interacts with transiently expressed α_{1A} P/Q-type Ca^{2+} channels and shifts the channels into a more inactivated state.

Unexpectedly, western blot analysis using a monoclonal antibody against human syntaxin-1A[25] showed that syntaxin-1A was not endogenously expressed in HEK293 cells (Fig. 2a); however, a 34–36 kilodalton band that co-migrated with syntaxin-1A protein was detected in HEK293 cells transfected with the α_{1A} P/Q-type Ca

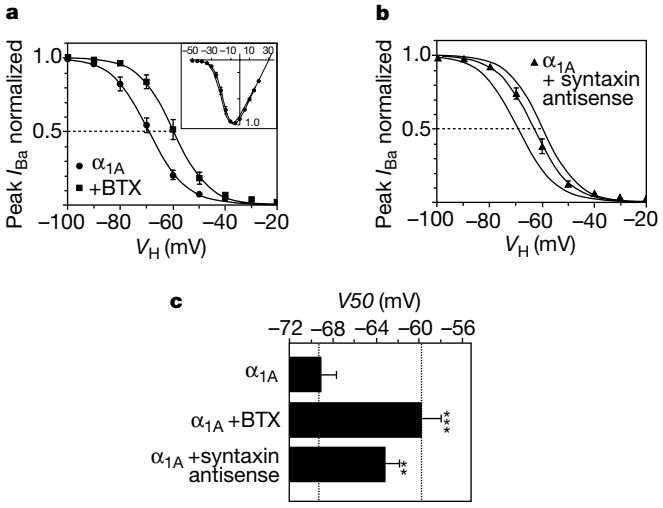

Figure 1 Interaction of syntaxin with α_{1A} P/Q-type channels induces a negative shift in steady-state inactivation (SSI). **a**, Cells were held at the holding voltage (V_H) for 15 s before activation; command voltage (V_c) = 0 mV. Data were normalized to the maximum current ($V_H = -120$ mV) and fitted using $y = 1/(1 + \exp((V50_{inact} - x)/k))$. Botulinum toxin (BTX) shifts $V50_{inact}$ to a more depolarized value without any change in the slope ($k = -5.6 \pm 0.2$, $P = 0.42$). **b**, Antisense syntaxin-1A induces a depolarizing shift in the SSI of α_{1A}. Dashed lines represent fits in (**a**). **c**, Summary of mean (±s.e.m.) $V50_{inact}$. ** = $P < 0.01$ and *** = $P < 0.001$ compared with α_{1A} control. I_{Ba}, maximum peak current.

channel. Polymerase chain reaction of reverse transcribed RNA (RT-PCR) also showed that syntaxin-1A messenger RNA was undetectable in untransfected HEK293 cells. In contrast, 24–36 h after transfection with α_{1A}, syntaxin-1A mRNA appeared and paralleled the expression of the exogenous P/Q-type Ca^{2+} channel (Fig. 2b). Syntaxin-1A mRNA was inhibited in transfected cells incubated in actinomycin D (2 μg ml^{-1}; data not shown), indicating that the P/Q-type response may involve transcriptional induction, although we cannot rule out affects on mRNA stability[26]. Co-transfection with only Ca^{2+} channel $\alpha_2\delta$ and β_{1b} subunits, CD8 vector and Bluescript plasmid did not induce syntaxin-1A expression (data not shown). Similarly, in α_{1A}-transfected cells RT-PCR did not show the expression of other SNARE proteins including syntaxin 1B, SNAP-25, synaptophysin, VAMP and synaptotagmin (data not shown).

To test whether functional P/Q-type Ca^{2+} channels were required to induce syntaxin-1A, we examined the effects of the selective P/Q-type channel antagonist ω-Agatoxin IVA (ω-Aga IVA). Figure 2c shows that syntaxin-1A mRNA was not induced in the presence of ω-Aga IVA (20 nM). Similar results were obtained when ω-Aga IVA was applied either at the time of α_{1A} transfection or 24 h after transfection (data not shown). Syntaxin-1A mRNA was also undetectable when ω-CTX MVIIC (200 nM) was applied just 4 h before cell harvesting, which implies the rapid turnover of syntaxin-1A mRNA (Fig. 2c). Furthermore, the presence of functional Ca^{2+} channels *per se* was not sufficient, as the transfection of other cloned Ca^{2+} channels, including α_{1B} (N-type), α_{1C} (L-type), α_{1E} (novel type) and the α_{1G} and α_{1I} T-type channels, did not result in detectable levels of syntaxin-1A mRNA (Fig. 2c). Stimulation of α_{1C} L-type Ca^{2+} channels with either 40 mM KCl or BAY-K8644 (10 μM) also failed to activate production of syntaxin-1A mRNA (data not shown). Thus, our data indicate that the selective functional expression of P/Q-type Ca^{2+} channels mediates the induction of syntaxin-1A.

The resting membrane potential of HEK293 cells in culture could conceivably allow a window current of Ca^{2+} influx through P/Q channels. Fura-2-based Ca^{2+} imaging showed that HEK293 cells transfected with α_{1A} Ca^{2+} channels (>48 h) exhibit elevated resting Ca^{2+} levels when compared with untransfected cells

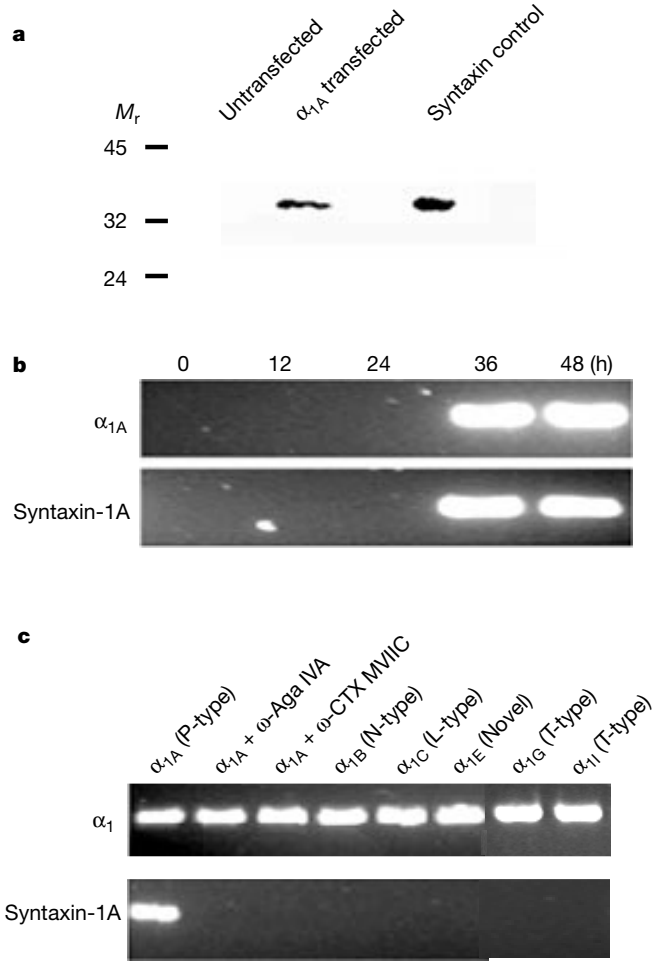

Figure 2 Functional α_{1A} P/Q channels stimulate the expression of syntaxin-1A. **a**, Western blot of control and transfected HEK293 cells shows syntaxin-1A protein after expression of α_{1A} channels. **b**, RT-PCR of HEK293 cells at increasing time intervals after transfection. Sequence analysis of the gel-eluted PCR product confirmed the identification of the PCR product as the human isoform syntaxin-1A mRNA (accession code L37792). **c**, The presence of either ω-Aga IVA or ω-CTX MVIIC during transfection and incubation of the cells prevents syntaxin-1A expression. Expression of α_{1B}, α_{1C}, α_{1E}, α_{1G} or α_{1I} Ca^{2+}-channel subtypes does not induce syntaxin-1A mRNA expression. M_r, relative molecular mass (×10^3).

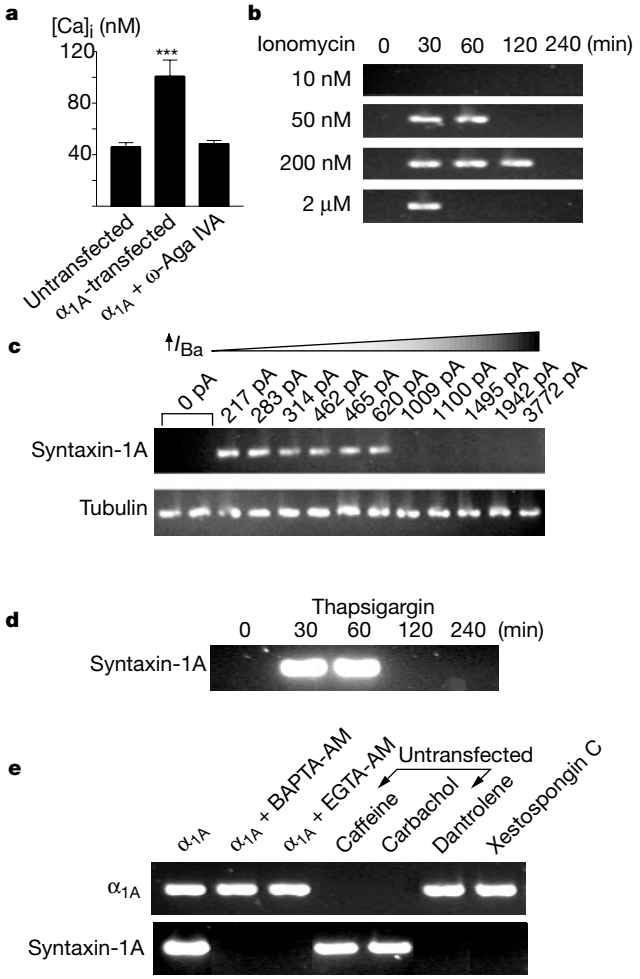

Figure 3 Syntaxin-1A expression is stimulated by distinct levels of intracellular Ca^{2+} and is mediated through activation of Ca^{2+} stores. **a**, $[Ca]_i$ levels are elevated in α_{1A}-transfected HEK293 cells; ***$P < 0.0001$. **b**, Ionomycin-induced Ca^{2+} influx activates syntaxin-1A expression in untransfected cells. **c**, Single-cell PCR and whole-cell P/Q-type currents of individual α_{1A} transfected cells. **d**, Thapsigargin transiently induces syntaxin-1A expression. **e**, Loading with BAPTA-AM or EGTA-AM (30 min at 2 μM) 4 h before harvesting blocks syntaxin-1A expression. Syntaxin-1A expression is stimulated in untransfected cells by release of Ca^{2+} from Ca^{2+} stores and blocked in α_{1A}-transfected cells when Ca^{2+} stores are inhibited.

(100.8 ± 12.6 nM and 46.1 ± 3.3 nM, respectively; $n = 67, 54$; Fig. 3a). Moreover, intracellular Ca^{2+} concentration returned to control levels when α_{1A}-transfected cells were incubated with ω-Aga IVA (48.7 ± 2.4 nM, $n = 34$), confirming that cultured HEK293 cells are subject to a basal Ca^{2+} current through exogenously expressed P/Q-type Ca^{2+} channels.

The requirement for extracellular Ca^{2+} was also investigated in untransfected cells using a 10-min application of ionomycin to produce a transient increase in intracellular Ca^{2+}. Applications of different concentrations of ionomycin (10 nM–2 μM) determined that syntaxin-1A expression exhibited a discrete upper and lower limit of Ca^{2+}-dependent activation with maximal activation occurring at relatively low levels of ionomycin (50–200 nM; Fig. 3b). Conversely, induction of syntaxin-1A mRNA in transfected cells was blocked when external Ca^{2+} was buffered using EGTA (2 mM; data not shown). The basal Ca^{2+} influx in α_{1A}-transfected cells raised the issue of whether the P/Q-type specificity of the syntaxin response was due to differences in expression levels for the different types of Ca^{2+} channel examined. Equivalent expression levels (measured as peak current amplitudes) for α_{1A}, α_{1B} and α_{1C} were investigated on a cell-by-cell basis and correlated with the presence or absence of syntaxin-1A mRNA using single cell RT-PCR. Figure 3c shows that only cells transfected with α_{1A} that exhibited currents within the range of ~200–600 pA induced syntaxin-1A ($n = 6$). In contrast, syntaxin-1A mRNA was undetectable in all the α_{1B} (N-type) and α_{1C} (L-type) transfected cells (peak current amplitudes ≈200–600 pA, $n = 4$ and 5, respectively; data not shown).

To map the intracellular regions that are effective in transducing the α_{1A}-specific Ca^{2+} influx, we tested a number of agents that alter intracellular Ca^{2+} levels ($[Ca]_i$). Release of Ca^{2+} from intracellular stores with a 10-min application of thapsigargin (10 μM) stimulated syntaxin-1A expression in untransfected cells (Fig. 3d). In α_{1A}-transfected cells both BAPTA-AM and EGTA-AM blocked the Ca^{2+}-dependent induction of syntaxin-1A (Fig. 3e). The slower Ca^{2+}-binding kinetics of EGTA (compared with BAPTA) limits its effective buffering capacity to regions more distal to the voltage-dependent Ca^{2+} influx[7]. Application of either caffeine (10 mM) or carbachol (20 μM) to activate Ca^{2+} release from ryanodine- and D-myo-inositol 1,4,5-trisphosphate (IP_3)-sensitive stores rapidly stimulated (<30 min) syntaxin-1A mRNA levels in untransfected cells (Fig. 3e). Conversely, block of either ryanodine-sensitive Ca^{2+} release with dantrolene (10 μM) or IP_3-induced Ca^{2+} release with Xestospongin C (1 μM)[27] inhibited α_{1A}-specific syntaxin-1A expression in transfected cells. Thus, a discrete level of basal α_{1A}-specific Ca influx induces syntaxin-1A expression through a secondary Ca^{2+} release from intracellular stores.

Ca^{2+}-dependent messengers and transcription factors such as CREB are important in initiating gene transcription[1,2]. Several different Ca^{2+}-dependent kinases and phosphatases, including calmodulin/Ca^{2+}-dependent (CaM) kinases I, II and IV, protein kinase A (PKA) and the Ras mitogen-activated kinase (MAPK) signalling pathway are responsible for regulating CREB activation[2,28,29]. Incubation of α_{1A}-transfected cells with calmidazolium (10 μM) to block calmodulin activity or KN-62 (900 nM), an inhibitor of CaM kinases II and IV, prevented syntaxin-1A expression (Fig. 4a). Incubation with H-9 (20 μM), H-8 (1 μM) or Rp-cAMP (10 μM) to inhibit PKA resulted in the block of syntaxin-1A expression in α_{1A}-transfected cells (Fig. 4a). Conversely, a 10-min application of the PKA activators forskolin (20 μM) or Sp-cAMPS (10 μM) induced syntaxin-1A mRNA in the absence of α_{1A} P/Q-type channels. Activation of protein kinase C with 12-*O*-tetradecanoylphorbol-13-acetate (TPA) did not induce expression in the absence of α_{1A} channels. Lastly, block of tyrosine kinase and MAPK kinase (MAPKK) activities by incubation with genistein (50 μM), and PD 098059 (50 μM), respectively, inhibited syntaxin-1A expression in α_{1A}-transfected cells, indicating that there may be involvement of the rsk kinase pathway.

Western blot analysis of control and α_{1A}-transfected cells showed

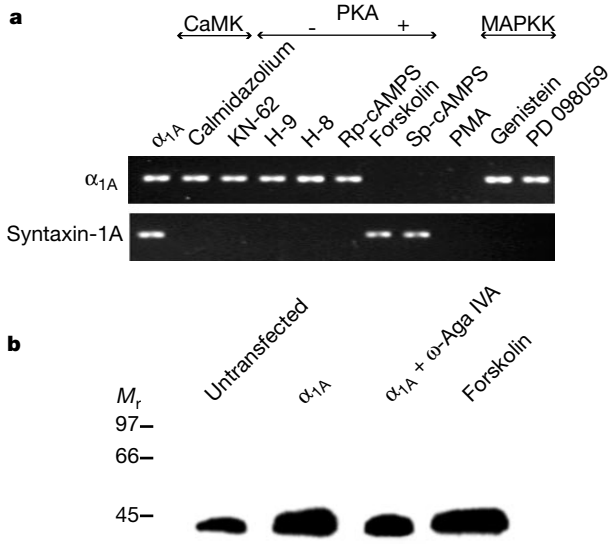

Figure 4 Involvement of second messengers in syntaxin-1A expression. **a**, Inhibition of calmodulin, CaM kinase II/IV or PKA blocks syntaxin-1A expression in α_{1A}-transfected cells. Stimulation of PKA with forskolin (20 μm) or Sp-cAMPS (10 μm) in untransfected cells activates expression (1 h after treatment). Activation of PKC with PMA (100 nM, 1 h) is ineffective, whereas incubation with genistein (50 μM) or PD 098059 blocks expression. **b**, Western blot for phosphorylated CREB. Lane 1, control HEK293 cell lysate; lane 2, α_{1A}-transfected HEK293 cells; lane 3, α_{1A} transfected HEK293 cells+ ω-Aga-IVA (20 nM, 10 h); lane 4, control HEK293 cells + 20 μM forskolin (30 min).

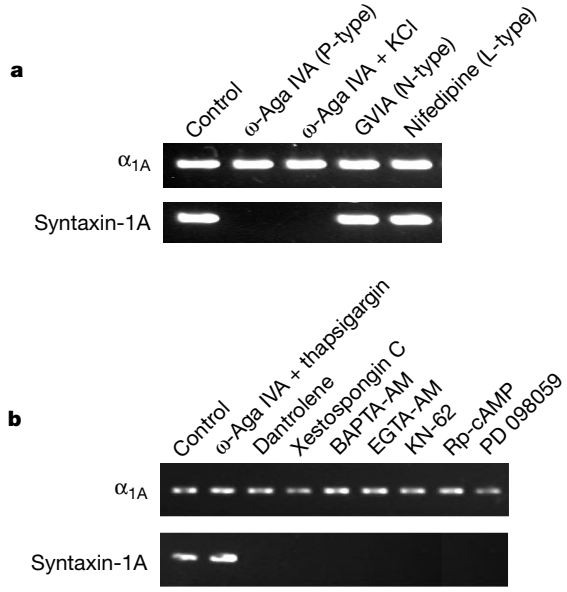

Figure 5 P/Q-type channels trigger syntaxin-1A expression in cerebellar granule neurons. **a**, RT-PCR from cultured cerebellar granule-cells. Block of P/Q-type channels (ω-Aga IVA, 100 nM) inhibits syntaxin-1A expression even in the presence of 40 mM KCl (30 min); inhibition of N-type channels with ω-CTx GVIA (1 μM) or L-type channels with nifedipine (10 μM) has no effect. **b**, Thapsigargin applied to granule cells (10 μM, 10 min) incubated in ω-Aga IVA (100 nM) reactivates syntaxin-1A expression. Dantrolene (10 μM), Xestospongin C (1 μM), BAPTA-AM (2 μM), EGTA-AM (2 μM), KN-62 (900 nM), Rp-CAMPS (10 μM) and PD 098059 (50 μM) block expression.

that the level of phosphorylated CREB is upregulated in HEK293 cells expressing functional α_{1A} Ca^{2+} channels (Fig. 4b). Moreover, the level of CREB phosphorylation is dependent upon Ca^{2+} influx through functional α_{1A} channels, as it returns to basal levels in the presence of ω-Aga IVA. Therefore, syntaxin-1A expression may be mediated by CREB, although the involvement of additional cofactors, such as CREB-binding protein, or Ca^{2+}-dependent transcription factors, such as DREAM, cannot be ruled out[2,10,11,30].

To correlate the results in transfected HEK293 cells with P/Q-type channels in neurons, syntaxin-1A expression was investigated in cultured cerebellar granule cells. RT-PCR of granule neurons showed that syntaxin-1A is basally expressed (Fig. 5a). Blockade of P/Q-type channels by incubation with ω-Aga IVA (100 nM) reduced syntaxin mRNA to undetectable levels, even in the presence of 40 mM KCl to maximize activation of Ca^{2+} channels insensitive to ω-Aga IVA. Moreover, inhibition of N- or L-type current with ω-CTx GVIA or nifedipine was ineffective at blocking the Ca^{2+}-dependent expression (Fig. 5a). Application of thapsigargin to granule cells incubated in ω-Aga IVA recovered syntaxin-1A expression (Fig. 5b). Furthermore, expression of syntaxin-1A was inhibited by blocking either ryanodine- or IP_3-induced Ca^{2+} release from stores, or by inhibiting CaM Kinase II/IV, PKA and MAPKK in a similar manner to that in HEK293 cells (Fig. 5b).

It is well established that Ca^{2+} influx through L-type Ca^{2+} channels stimulates CREB-activated gene expression[6–11]. Our results show that discrete levels of Ca^{2+} influx through P/Q-type channels provides an alternative means of mediating Ca^{2+}-dependent gene expression. P/Q-type-selective Ca^{2+} influx induces the expression of syntaxin-1A and not of other SNARE proteins involved in vesicle fusion and neurotransmitter release. The regulation of syntaxin-1A appears to be under tight spatial and temporal Ca^{2+}-dependent control and is similar to that for the Ca^{2+}-dependent expression of other genes[4,5]. This finding, coupled with a supporting role for Ca^{2+} release from intracellular stores, indicates that there may be a privileged close association between P/Q-type channels and Ca^{2+} stores. The induced syntaxin-1A protein appears to act as a negative feedback regulator of P/Q-type channels and may have a critical role in modulating synaptic activity. □

Methods

Electrophysiology and cell culture

HEK293 tsa201 cells were transiently transfected with Ca^{2+}-channel subunits using standard Ca^{2+}-phosphate precipitation. Human α_{1A} (P/Q-type), rat α_{1B} (N-type), rat α_{1C} (L-type) and rat α_{1E} (novel type) Ca^{2+}-channel subunits (1–3 μg of complementary DNA) were co-transfected with rat $\alpha_2\delta$ and β_{1b} ancillary subunits (molar ratio 1:1:1), 2 μg of CD8 marker plasmid and 9–15 μg Bluescript SK carrier DNA (total = 20 μg cDNA per transfection). The α_{1G} and α_{1I} T-type Ca^{2+}-channel subunits were transfected without Ca^{2+}-channel ancillary subunits. Whole-cell patch clamp recordings were performed 48–96 h after transfection. The internal patch-pipette solution contained (in mM): 105 CsCl, 25 TEACl, 1 $CaCl_2$, 11 EGTA, 10 HEPES, pH 7.2. The external recording solution contained (in mM): 5 $BaCl_2$, 1 $MgCl_2$, 10 HEPES, 40 TEACl, 10 Glucose, 87.5 CsCl, pH 7.2. Currents were typically elicited from a holding potential of −120 mV to maximize the availability of syntaxin-1A-bound α_{1A} channels[20]. Data were filtered at 1 kHz and in most cases subtraction of capacitance and leakage currents was carried out on-line using a P/4 protocol.

Cerebellar granule cells were prepared from 7-day rat pups by incubation of cerebellar pieces with trypsin solution (0.025% trypsin, 0.25% glucose, 0.3% BSA, 35 mM $MgSO_4$) at 37 °C for 20 min and treatment with DNase I (1 mg ml^{-1} in 0.1 mg ml^{-1} trypsin inhibitor and 35 mM $MgSO_4$); cells were collected by centrifugation. After trituration and pelleting, cells were incubated at 37 °C in MEM + 10% FCS for 24 h and then in MEM + 10% FCS+ 5 fluoro 5′-deoxyuridine.

RNA preparation and RT-PCR

For each experiment, approximately 10^6 HEK293 cells were harvested 48 h after transfection and resuspended in 1 ml of extraction buffer (4M guanidinium thiocyanate, 20 μl β mercaptoethanol, 100 μl of Na-acetate pH 4.0), 1 ml H_2O-saturated phenol and 200 μl chloroform. Unless otherwise stated, all inhibitory agents were added 4 h before harvesting. After isolation of RNA, reverse transcriptase reactions were performed with 1 μg total RNA and 20 pmol of a 3′ oligonucleotide (antisense). The syntaxin-1A 3′ oligonucleotide corresponds to basepairs (bp) 860–841 of the human syntaxin-1A mRNA sequence (accession code M95734). Other 3′ antisense oligonucleotides utilized included syntaxin 1B bp 749–769 (accession code 4507290); synaptophysin bp 919–902 (accession code X06389); synaptotagmin bp 1,783–1,765 (accession code M55047); VAMP bp 279–262 pb (accession code AF060538); SNAP-25 bp 453–436 (accession code L19760), α_{1A} Ca^{2+} channel bp 1,262–1,244 (accession code M64373); and α-tubulin bp 738–721 (accession code V01227). RNA and 3′ oligonucleotides were heated to 90 °C for 10 min, placed on ice and a mixture of 1 × RT buffer, 10 mM dNTPs, 100 mM DTT and 5 units of Superscript RT (Gibco BRL) was added to a final volume of 20 μl. Reactions were mixed and incubated at 42 °C for 1.5 h.

PCR was carried out with 5 μl of the RT mix, 20 pmol of each 5′ and 3′ oligonucleotide, 10 mM dNTPs, 2.5 mM $MgCl_2$ and 2 units of TAQ polymerase to a final volume of 50 μl. The human syntaxin-1A 5′ oligonucleotide utilized corresponds to bp 241–258; syntaxin-1B to bp 342–362; synaptophysin to bp 556–574; synaptotagmin to bp 799–816; VAMP to bp 34–52; SNAP-25 to bp 89–106; α_{1A} P/Q-type to bp 652–670; and α-tubulin to bp 592–612. The PCR cycling parameters were 92 °C (1 min), 50 °C (1.25 min), 74 °C (1 min) for 10 cycles, followed by 92 °C (1 min), 57 °C (0.75 min), 74 °C (1 min) for 20 cycles. To confirm the identity of syntaxin-1A, PCR reactions were separated routinely through a 1.3% agarose gel, transferred to a Nytran membrane and probed with a radiolabelled syntaxin-1A-specific oligonucleotide.

For single-cell PCR experiments, the RT and PCR protocols were as described above except that cell contents were drawn into the recording pipette and added to 12 μl of the RT mix without reverse transcriptase. One half of the RT mix was used for the syntaxin-1A PCR and the other half for either tubulin or Ca^{2+}-channel α_1-subunit PCR.

Calcium imaging

Calcium imaging was performed using 17 μM fura-2 AM loaded into HEK293 cells (30 min, room temperature in 0.067% pluronic). Resting $[Ca]_i$ was estimated by taking 380/360 nm excitation image pairs (isosbestic point ratio) in DMEM culture medium that was equilibrated with a 5% CO_2/95% air mixture and continuously perfused. Ratio values were converted to $[Ca^{2+}]_i$ values based on parameters obtained from an *in vitro* calibration.

Western blot

For each experiment, approximately 10^6 HEK293 cells were harvested 48 h after transfection and lysed directly into loading buffer (4% SDS, 20% glycerol, 0.12 M Tris pH 6.8, 0.01% bromophenol blue, 0.1% DTT). Samples were boiled and proteins separated by electrophoresis through a 12% SDS-PAGE gel before transfer to a nylon filter (Nytran). Blots were probed with primary antibodies against the phosphorylated form of CREB (pCREB, Upstate Biotechnology) or human syntaxin (SP8, gift of W. Honer), and secondary antibody (anti-mouse Ig, Amersham) before bands were visualized using a commercial ECL detection kit (Amersham).

Received 4 May; accepted 26 August 1999.

1. Ghosh, A. & Greenburg, M. E. Calcium signalling in neurons: molecular mechanisms and cellular consequences. *Science* **268,** 239–247 (1995).
2. Bito, H., Deisseroth, K. & Tsien, R. W. Ca2+-dependent regulation in neuronal gene expression. *Curr. Opin. Neurobiol.* **7,** 419–429 (1997).
3. Hardingham, G. E., Chawla, S., Johnson, C. M. & Bading, H. Distinct functions of nuclear and cytoplasmic calcium in the control of gene expression. *Nature* **385,** 260–265 (1997).
4. Dolmetsch, R. E., Lewis, R. S., Goodnow, C. C. & Healy, J. I. Differential activation of transcription factors induced by Ca^{2+} response amplitude and duration. *Nature* **386,** 855–858 (1997).
5. Li, W., Llopis, J., Whitney, M., Zlokarnik, G. & Tsien, R. Y. Cell-permeant caged $InsP_3$ ester shows that Ca^{2+} spike frequency can optimize gene expression. *Nature* **392,** 936–941 (1998).
6. Bading, H., Ginty, D. D. & Greenberg, M. E. Regulation of gene expression in hippocampal neurons by distinct calcium signaling pathways. *Science* **260,** 181–186 (1993).
7. Deisseroth, K., Bito, H. & Tsien, R. W. Signalling from synapse to nucleus: postsynaptic CREB phosphorylation during multiple forms of hippocampal synaptic plasticity. *Neuron* **16,** 89–101 (1996).
8. Bito, H., Deisseroth, K. & Tsien, R. W. CREB phosphorylation and dephosphorylation: a Ca2+- and stimulus duration-dependent switch for hippocampal gene expression. *Cell* **87,** 1203–1214 (1996).
9. Diesseroth, K., Heist, E. K. & Tsien, R. W. Translocation of calmodulin to the nucleus supports CREB phosphorylation in hippocampal neurons. *Nature* **392,** 198–202 (1998).
10. Tao, X., Finkbeiner, S., Arnold, D. B., Shaywitz, A. J. & Greenberg, M. E. Ca^{2+} influx regulates BDNF transcription by a CREB family transcription factor-dependent mechanism. *Neuron* **20,** 709–726 (1998).
11. Shieh, P. B., Hu, S.-C., Bobb, K., Timusk, T. & Ghosh, A. Identification of a signaling pathway involved in calcium regulation of BDNF expression. *Neuron* **20,** 727–740 (1998).
12. Llina, R., Sugimori, M., Lin, J. W. & Cherksey, B. Blocking and isolation of a calcium channel from neurons in mammals and cephalopods utilizing a toxin fraction (FTX) from funnel-web spider poison. *Proc. Natl Acad. Sci. USA* **86,** 1689–1693 (1989).
13. Mintz, I. M., Adams, M. E. & Bean, B. P. P-type calcium channels in rat central and peripheral neurons. *Neuron* **9,** 85–95 (1992).
14. Bourinet, E. *et al.* Splicing of α_{1A} subunit gene generates phenotypic variants of P- and Q-type calcium channels. *Nature Neurosci.* **2,** 407–415 (1999).
15. Betz, A., Okamoto, M., Benseler, F. & Brose, N. Direct interaction of the rat unc-13 homologue munc13-1 with the N-terminus of syntaxin. *J. Biol. Chem.* **272,** 2520–2526 (1997).
16. Pevsner, J. *et al.* Specificity and regulation of a synaptic vesicle docking complex. *Neuron* **13,** 353–361 (1994).
17. Fujita, Y. *et al.* Tomosyn: a syntaxin-1-binding protein that forms a novel complex in the neurotransmitter release process. *Neuron* **20,** 905–915 (1998).
18. Sheng, Z.-H., Westenbroek, R. E. & Catterall, W. A. Physical link and functional coupling of presynaptic calcium channels and the synaptic vesicle docking/fusion machinery. *J. Bioenerg. Biomembr.* **30,** 335–345 (1998).

19. Sheng, Z.-H., Rettig, J., Takahashi, M. & Catterall, W. A. Identification of a syntaxin-binding site on N-type calcium channels. *Neuron* **13,** 1303–1313 (1994).
20. Bezprozvanny, I., Scheller, R. H. & Tsien, R. W. Functional impact of syntaxin on gating of N-type and Q-type calcium channels. *Nature* **378,** 623–626 (1995).
21. Martin-Moutot, N. *et al.* Interaction of SNARE complexes with P/Q-type calcium channels in rat cerebellar synaptosomes. *J. Biol. Chem.* **271,** 6567–6570 (1996).
22. Rettig, J. *et al.* Isoform-specific interaction of the α_{1A} subunits of brain Ca^{2+} channels with the presynaptic proteins syntaxin and SNAP-25. *Proc. Natl Acad. Sci. USA* **93,** 7363–7368 (1996).
23. Kim, D. K. & Catterall, W. A. Ca^{2+}-dependent and -independent interactions of the isoforms of the α_{1A} subunit of brain Ca^{2+} channels with presynaptic SNARE proteins. *Proc. Natl Acad. Sci. USA* **94,** 14782–14786 (1997).
24. Williamson, L. C., Halpern, J. L., Montecucco, C., Brown, J. E. & Neale, E. A. Clostridial neurotoxins and substrate proteolysis in intact neurons: botulinum neurotoxin C acts on synaptosomal-associated protein of 25 kDa. *J. Biol. Chem.* **271,** 7694–7699 (1996).
25. Honer, W. G., Hu, L, & Davies, P. Human synaptic proteins with a heterogenous distribution in cerebellum and visual cortex. *Brain Res.* **609,** 9–20 (1993).
26. Daly, C. & Ziff, E. B. Post-transcriptional regulation of synaptic vesicle protein expression and the developmental control of synaptic vesicle formation. *J. Neurosci.* **17,** 2365–2375 (1997).
27. Gafni, J. *et al.* Xestospongins: potent membrane permeable blockers of the inositol 1,4,5-trisphosphate receptor. *Neuron* **19,** 723–733 (1997).
28. Gonzalez, G. A. & Montminy, M. R. Cyclic AMP stimulates somatostatin gene transcription by phosphorylation of CREB at serine 133. *Cell* **59,** 675–680 (1989).
29. Ginty, D. D., Bonni, A. & Greenberg, M. E. Nerve growth factor activates a Ras-dependent protein kinase that stimulates c-fos transcription via phosphorylation of CREB. *Cell* **77,** 713–725 (1994).
30. Carrion, A. M., Link, W. A., Ledo, F., Mellstrom, B. & Naranjo, J. R. DREAM is a Ca^{2+}-regulated transcriptional repressor. *Nature* **398,** 80–84 (1999).

Acknowledgements

We thank M. Gilbert, C. Santi, A. Stea and G. Zamponi for comments and discussions. We also thank W. Honer for providing the SP8 human syntaxin-1A monoclonal antibody and D. Brink and V. Leuranguer for tissue culture support. The research was supported by grants from the Medical Research Council (MRC) of Canada (T.P.S. and T.H.M.), postdoctoral support from the Amyotrophic Lateral Sclerosis Society of Canada (K.S.), and studentship and postdoctoral fellowship support from the MRC (H.G. and J.M., respectively). T.P.S. and T.H.M. are recipients of MRC of Canada Scientist awards.

Correspondence and requests for materials should be addressed to T.P.S. (e-mail: snutch@zoology.ubc.ca).

Extraintestinal dissemination of *Salmonella* by CD18-expressing phagocytes

Andrés Vazquez-Torres*, Jessica Jones-Carson†, Andreas J. Bäumler‡, Stanley Falkow§, Raphael Valdivia§‖, William Brown*¶, Mysan Le*¶, Ruth Berggren*‖, W. Tony Parks# & Ferric C. Fang*

** Departments of Medicine, Pathology, and Microbiology, University of Colorado Health Sciences Center, Denver, Colorado 80262, USA*
† Department of Immunology, National Jewish Center for Immunology and Respiratory Medicine, Denver, Colorado 80262, USA
‡ Department of Medical Microbiology and Immunology, Texas A&M University, College Station, Texas 77843-1114, USA
§ Department of Microbiology and Immunology, Stanford University School of Medicine, Stanford, California 94305, USA
¶ Department of Medicine, Veterans Affairs Medical Center, Denver, Colorado 80262, USA
 # Laboratory of Cell Regulation and Carcinogenesis, National Cancer Institute, National Institutes of Health, Bethesda, Maryland 20892, USA

Specialized epithelia known as M cells overlying the lymphoid follicles of Peyer's patches are important in the mucosal immune system, but also provide a portal of entry for pathogens such as *Salmonella typhimurium*, *Mycobacterium bovis*, *Shigella flexneri*, *Yersinia enterocolitica* and reoviruses[1–4]. Penetration of intestinal M cells and epithelial cells by *Salmonella typhimurium* requires the invasion genes of *Salmonella* Pathogenicity Island 1 (SPI1)[3,5–9]. SPI1-deficient *S. typhimurium* strains gain access to the spleen following oral administration and cause lethal infection in mice[5] without invading M cells[3,9] or localizing in Peyer's patches[10], which indicates that *Salmonella* uses an alternative strategy to disseminate from the gastrointestinal tract. Here we report that *Salmonella* is transported from the gastrointestinal tract to the bloodstream by CD18-expressing phagocytes, and that CD18-deficient mice are resistant to dissemination of *Salmonella* to the liver and spleen after oral administration. This CD18-dependent pathway of extraintestinal dissemination may be important for the development of systemic immunity to gastrointestinal pathogens, because oral challenge with SPI1-deficient *S. typhimurium* elicits a specific systemic IgG humoral immune response, despite an inability to stimulate production of specific mucosal IgA.

As phagocytic cells transmigrate across normal tissue barriers[11] and *Salmonella* can survive within mononuclear phagocytic cells[12], we proposed that tissue macrophages transport *Salmonella* from the intestine to the systemic circulation; CD18-deficient mice[13] provided a model in which to test this hypothesis. Among its many functions, the β2-integrin CD18 mediates leukocyte transmigration in response to various stimuli, including *S. typhimurium*[14,15].

We introduced mutations in the *invA* gene into wild-type *S. typhimurium* ATCC 14028s to inactivate the SPI1 invasion genes, and added a mutation in the *lpfC* fimbrial gene[16] to impair targeting of Peyer's patches further. An *aroA* mutation in the gene encoding 3-enol-pyruvylshikimate synthase was incorporated to reduce virulence and allow the survival of infected animals. CD18-deficient mice infected orally with the *invA–lpfC–aroA* mutant *S. typhimurium* strain harboured 100-fold fewer bacteria in the spleen and liver than did similarly infected congenic C57BL/6 controls (Fig. 1a). The resistance of CD18-deficient mice to *Salmonella* dissemination from the gastrointestinal tract cannot be explained by enhanced bacterial clearance from systemic sites, because the CD18-deficient mouse strain was found to be more susceptible than congenic C57BL/6 mice to splenic and hepatic infection following intraperitoneal challenge with *invA–lpfC–aroA* mutant *S. typhimurium* (Fig. 1b). Moreover, periodate-elicited peritoneal macrophages from CD18-deficient mice were less efficient at killing *Salmonella in vitro* than control macrophages from C57BL/6 mice (data not shown). These observations indicate that a CD18-dependent host process may enable *S. typhimurium* to

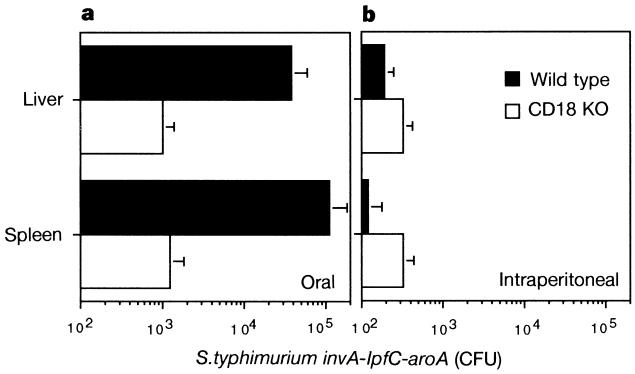

Figure 1 CD18-dependent dissemination of invasion-deficient *S. typhimurium* from the gastrointestinal tract to systemic organs. CD18 β2 integrin-deficient mice are more resistant than congenic C57BL/6 controls to systemic dissemination of *invA–lpfC–aroA* mutant bacteria following oral (**a**) but not intraperitoneal (**b**) inoculation. The spleens of C57BL/6 mice contain 100-fold more bacteria than those from CD18-deficient controls after oral administration, but 2–3-fold fewer bacteria after intraperitoneal inoculation. The data represent the mean ± s.e.m. of 5–10 mice from two independent experiments.

‖ Present addresses: Department of Biochemistry, University of California at Berkeley, Berkeley, California 94720, USA (R.V.); Department of Medicine, University of Texas Southwestern Medical Center, Dallas, Texas 75325, USA (R.B.).